

# Future sea level change under CMIP5 and CMIP6 scenarios from the Greenland and Antarctic ice sheets

3 Antony J. Payne <sup>1</sup>, Sophie Nowicki <sup>2,3</sup>, Ayako Abe-Ouchi <sup>4</sup>, Cécile Agosta <sup>5</sup>,  
 4 Patrick Alexander <sup>6,7</sup>, Torsten Albrecht <sup>8</sup>, Xylar Asay-Davis <sup>9</sup>, Andy  
 5 Aschwanden <sup>10</sup>, Alice Barthel <sup>9</sup>, Thomas J. Bracegirdle <sup>11</sup>, Reinhard Calov <sup>8</sup>,  
 6 Christopher Chambers <sup>12</sup>, Youngmin Choi <sup>13</sup>, Richard Cullather <sup>2</sup>, Joshua  
 7 Cuzzone <sup>14</sup>, Christophe Dumas <sup>5</sup>, Tamsin L. Edwards <sup>15</sup>, Denis Felikson <sup>2,16</sup>,  
 8 Xavier Fettweis <sup>17</sup>, Benjamin K. Galton-Fenzi <sup>18,19</sup>, Heiko Goelzer <sup>20,21,22</sup>,  
 9 Rupert Gladstone <sup>23</sup>, Nicholas R. Golledge <sup>24</sup>, Jonathan M. Gregory <sup>25,26</sup>, Ralf  
 10 Greve <sup>11,27</sup>, Tore Hattermann <sup>28,29</sup>, Matthew J. Hoffman <sup>9</sup>, Angelika Humbert  
 11 <sup>30,31</sup>, Philippe Huybrechts <sup>32</sup>, Nicolas C. Jourdain <sup>33</sup>, Thomas Kleiner <sup>30</sup>, Peter  
 12 Kuipers Munneke <sup>20</sup>, Eric Larour <sup>14</sup>, Sébastien Le clec'h <sup>32</sup>, Victoria Lee <sup>1</sup>,  
 13 Gunter Leguy <sup>34</sup>, William H. Lipscomb <sup>34</sup>, Christopher M. Little <sup>35</sup>, Daniel P.  
 14 Lowry <sup>36</sup>, Mathieu Morlighem <sup>13</sup>, Isabel Nias <sup>2,37</sup>, Frank Pattyn <sup>21</sup>, Tyler Pelle  
 15 <sup>13</sup>, Stephen F. Price <sup>9</sup>, Aurélien Quiquet <sup>5</sup>, Ronja Reese <sup>8</sup>, Martin Rückamp  
 16 <sup>30</sup>, Nicole-Jeanne Schlegel <sup>14</sup>, Hélène Seroussi <sup>14</sup>, Andrew Shepherd <sup>38</sup>, Erika  
 17 Simon <sup>2</sup>, Donald Slater <sup>39</sup>, Robin S. Smith <sup>25</sup>, Fiammetta Straneo <sup>39</sup>, Sainan  
 18 Sun <sup>21</sup>, Lev Tarasov <sup>40</sup>, Luke D. Trusel <sup>41</sup>, Jonas Van Breedam <sup>32</sup>, Roderik van  
 19 de Wal <sup>20,42</sup>, Michiel van den Broeke <sup>20</sup>, Ricarda Winkelmann <sup>8,43</sup>, Chen Zhao  
 20 <sup>19</sup>, Tong Zhang <sup>9</sup>, Thomas Zwinger <sup>44</sup>

<sup>21</sup><sup>1</sup>Centre for Polar Observation and Modelling, University of Bristol, Bristol, UK

<sup>22</sup><sup>2</sup>Cryospheric Sciences Laboratory, Code 615, NASA Goddard Space Flight Center, Greenbelt, MD 20771,

USA

<sup>23</sup><sup>3</sup>Geology Department and RENEW Institute, University at Buffalo, Buffalo, NY, USA

<sup>24</sup><sup>4</sup>Atmosphere and Ocean Research Institute, The University of Tokyo, Kashiwa-shi, Japan

<sup>25</sup><sup>5</sup>Laboratoire des Sciences du Climat et de l'Environnement, LSCE-IPSL, CEA-CNRS-UVSQ, Université

Paris-Saclay, Gif-sur-Yvette, France

<sup>26</sup><sup>6</sup>Lamont-Doherty Earth Observatory, Columbia University, Palisades, NY, USA

<sup>27</sup><sup>7</sup>NASA Goddard Institute for Space Studies, New York, NY, USA

<sup>28</sup><sup>8</sup>Potsdam Institute for Climate Impact Research (PIK), Member of the Leibniz Association, Potsdam,

Germany

<sup>29</sup><sup>9</sup>Theoretical Division, Los Alamos National Laboratory, Los Alamos, NM, USA

<sup>30</sup><sup>10</sup>Geophysical Institute, University of Alaska, Fairbanks, AK 99775, USA

<sup>31</sup><sup>11</sup>British Antarctic Survey, Cambridge, UK

<sup>32</sup><sup>12</sup>Institute of Low Temperature Science, Hokkaido University, Sapporo, Japan

<sup>33</sup><sup>13</sup>Department of Earth System Science, University of California Irvine, Irvine, USA

<sup>34</sup><sup>14</sup>Jet Propulsion Laboratory, California Institute of Technology, Pasadena, CA, USA

<sup>35</sup><sup>15</sup>Department of Geography, King's College London, London, UK

<sup>36</sup><sup>16</sup>Universities Space Research Association, Goddard Earth Sciences Technology and Research Studies and

Investigations, Columbia, MD 21044, USA

<sup>37</sup><sup>17</sup>Laboratory of Climatology, Department of Geography, University of Liège, Liège, Belgium

<sup>38</sup><sup>18</sup>Australian Antarctic Division, Kingston, Tasmania, Australia

<sup>39</sup><sup>19</sup>Australian Antarctic Program Partnership, Institute for Marine and Antarctic Studies, University of

Tasmania, Hobart, Tasmania, Australia

<sup>40</sup><sup>20</sup>Institute for Marine and Atmospheric research Utrecht, Utrecht University, Utrecht, the Netherlands

<sup>41</sup><sup>21</sup>Laboratoire de Glaciologie, Université Libre de Bruxelles, Brussels, Belgium

<sup>42</sup><sup>22</sup>NORCE Norwegian Research Centre, Bjerknes Centre for Climate Research, Bergen, Norway

<sup>43</sup><sup>23</sup>Arctic Centre, University of Lapland, Finland

<sup>44</sup><sup>24</sup>Antarctic Research Centre, Victoria University of Wellington, New Zealand

<sup>45</sup><sup>25</sup>National Center for Atmospheric Science, University of Reading, Reading, UK

<sup>46</sup><sup>26</sup>Met Office, Hadley Centre, Exeter, UK

<sup>47</sup><sup>27</sup>Arctic Research Center, Hokkaido University, Sapporo, Japan

<sup>48</sup><sup>28</sup>Norwegian Polar Institute, Tromsø, Norway

<sup>49</sup><sup>29</sup>Department of Physics and Technology, The Arctic University University of Tromsø, Norway

<sup>50</sup><sup>30</sup>Alfred Wegener Institute for Polar and Marine Research, Bremerhaven, Germany

<sup>51</sup><sup>31</sup>Department of Geoscience, University of Bremen, Bremen, Germany

<sup>52</sup><sup>32</sup>Earth System Science and Departement Geografie, Vrije Universiteit Brussel, Brussels, Belgium

<sup>53</sup><sup>33</sup>Univ. Grenoble Alpes/CNRS/IRD/G-INP, Institut des Géosciences de l'Environnement, France

<sup>54</sup><sup>34</sup>Climate and Global Dynamics Laboratory, National Center for Atmospheric Research, Boulder, CO,

USA

<sup>55</sup><sup>35</sup>Atmospheric and Environmental Research, Inc., Lexington, Massachusetts, USA

<sup>56</sup><sup>36</sup>GNS Science, Lower Hutt, New Zealand

<sup>57</sup><sup>37</sup>School of Environmental Sciences, University of Liverpool, Liverpool, UK

<sup>58</sup><sup>38</sup>Centre for Polar Observation and Modelling, University of Leeds, LS2 9JT, UK

<sup>39</sup>Scripps Institution of Oceanography, University of California San Diego, La Jolla, CA, USA  
<sup>40</sup>Dept of Physics and Physical Oceanography, Memorial University of Newfoundland, Canada  
<sup>41</sup>Department of Geography, Pennsylvania State University, University Park, PA, USA  
<sup>42</sup>Geosciences, Physical Geography, Utrecht University, Utrecht, The Netherlands  
<sup>43</sup>Department of Physics and Astronomy, University of Potsdam, Potsdam, Germany  
<sup>44</sup>CSC-IT Center for Science, Espoo, Finland

71

## Key Points:

- We compare results from an ice sheet model inter-comparison forced using CMIP6 and CMIP5 climate projections
  - Projected sea level at 2100 is higher for Greenland under CMIP6 scenarios than CMIP5, but similar for Antarctica under both scenarios
  - CMIP6 warmer climate results in increased Greenland surface melt while increased snowfall mitigates loss from ocean warming for Antarctica

Corresponding author: Tony Payne and Sophie Nowicki, [a.j.payne@bristol.ac.uk](mailto:a.j.payne@bristol.ac.uk)  
[sophien@buffalo.edu](mailto:sophien@buffalo.edu)

78 **Abstract**

79 Projections of the sea level contribution from the Greenland and Antarctic ice sheets rely  
 80 on atmospheric and oceanic drivers obtained from climate models. The Earth System  
 81 Models participating in the Coupled Model Intercomparison Project phase 6 (CMIP6)  
 82 generally project greater future warming compared with the previous CMIP5 effort. Here  
 83 we use four CMIP6 models and a selection of CMIP5 models to force multiple ice sheet  
 84 models as part of the Ice Sheet Model Intercomparison Project for CMIP6 (ISMIP6).  
 85 We find that the projected sea level contribution at 2100 from the ice sheet model en-  
 86 semble under the CMIP6 scenarios falls within the CMIP5 range for the Antarctic ice  
 87 sheet but is significantly increased for Greenland. Warmer atmosphere in CMIP6 mod-  
 88 els results in higher Greenland mass loss due to surface melt. For Antarctica, CMIP6  
 89 forcing is similar to CMIP5 and mass gain from increased snowfall counteracts increased  
 90 loss due to ocean warming.

91 **Plain Language Summary**

92 The melting of the Greenland and Antarctic ice sheets will result in higher sea level  
 93 in the future. How sea level will change depends in part on how the atmosphere and ocean  
 94 warm and how this affects the ice sheets. We use multiple ice sheet models to estimate  
 95 possible future sea levels under climate scenarios from the models participating in the  
 96 new Coupled Model Intercomparison Project phase 6 (CMIP6), which generally indicate  
 97 a warmer world than the previous effort (CMIP5). Our results show that the possible  
 98 future sea level change due to Antarctica is similar for CMIP5 and CMIP6, but the warmer  
 99 atmosphere in CMIP6 models leads to higher sea-level contributions from Greenland by  
 100 the end of the century.

101 **1 Introduction**

102 The overall aim of this paper is to assess whether the stronger future warming shown  
 103 by many CMIP6 models (Forster et al., 2019; Meehl et al., 2020) compared with CMIP5  
 104 has a significant impact on future Global Mean Sea Level Rise (GMSLR). We compare  
 105 projections for the sea-level contribution of the Greenland and Antarctic ice sheets (GrIS  
 106 and AIS) under climate forcing from a small group of models from the CMIP6 ensem-  
 107 ble (Eyring et al., 2016) with that of models using forcing from the CMIP5 model en-  
 108 semble (Taylor et al., 2012). Goelzer et al. (2020b) and Seroussi et al. (2020) present de-  
 109 tailed analyses of the latter set of experiments for GrIS and AIS, respectively. In both  
 110 cases, a great deal of attention was paid to sampling the CMIP5 ensemble effectively,  
 111 so that the CMIP5 models used to provide climate forcing both represented the present-  
 112 day climate of the ice sheets well and sampled the range of future projections of the over-  
 113 all ensemble. Details of this procedure can be found in Barthel et al. (2020).

114 Global warming as manifested in regional atmospheric and oceanic change can im-  
 115 pact the ice sheet mass budget, and hence contribution to GMSLR, in a number of ways.  
 116 Warming of the atmosphere over the ice sheet promotes increased melt from snow and  
 117 ice surfaces leading to increased mass loss in the form of runoff to the oceans. It may  
 118 also be associated with increased precipitation because of the increased moisture-carrying  
 119 capacity of warmer air. The relationship between global warming and the warmth of Po-  
 120 lar ocean water masses impinging on the ice sheets is likely to be more complex. The warm-  
 121 ing of these water masses is expected to increase GMSLR by increasing mass loss from  
 122 the marine-terminating outlet glaciers of the GrIS, and by processes associated with Ma-  
 123 rine Ice Sheet Instability (Schoof, 2007) for the AIS. An additional complexity for GrIS  
 124 is that marine mass loss is partly controlled by freshwater fluxes from the surface melt  
 125 (Slater et al., 2019). Finally, Marine Ice Sheet Instability could also be triggered by at-  
 126 mospheric warming leading to the fracture and collapse of floating ice shelves (Trusel et  
 127 al., 2015). This process may in turn lead to the subsequent rapid retreat of the exposed

128 marine ice cliffs (DeConto & Pollard, 2016). In summary, the range and complexity of  
 129 the ways in which climate affects ice-sheet mass budget suggests that the greater global  
 130 warming found in CMIP6 models may not necessarily lead to increased GMSLR.

## 131 2 The CMIP6 ensemble

132 We compare a small ensemble of four Earth System Models (ESMs) submitted to  
 133 the CMIP6 exercise. These models are UKESM1-0-LL, CESM2, CNRM-CM6-1 and CNRM-  
 134 ESM2-1. Because the sample is small and based on availability only, it is important to  
 135 understand the difference between the selected models and the larger CMIP6 model en-  
 136 semble. Effective Climate Sensitivity (ECS)(IPCC, 2013) is a convenient measure of this.  
 137 ECS estimates the global mean temperature response to doubled atmospheric carbon  
 138 dioxide concentration (Flato et al., 2013). The four selected models all have ECS at the  
 139 upper end of the CMIP6 ensemble (CESM2, CNRM-CM6-1, CNRM-ESM2-1 and UKESM1-  
 140 0-LL have ECS of 5.2, 4.8, 4.8 and 5.3 °C, respectively). Roughly half of the CMIP6 en-  
 141 semble has an ECS of between 4.6 and 5.6 °C, while there is a second similarly-sized group  
 142 with markedly lower ECS in the range 2.3 to 3.2 °C (Meehl et al., 2020). In contrast,  
 143 the CMIP5 ensemble exhibited a fairly continuous range of ECS between 2.1 and 4.7 °C  
 144 (Flato et al., 2013). The CMIP5 models used in Goelzer et al. (2020b) and Seroussi et  
 145 al. (2020) were typically drawn from the upper end of this distribution (e.g., MIROC-  
 146 ESM, HadGEM2-ES, CSIRO-Mk3-6-0 and IPSL-CM5A-LR with ECS of 4.7, 4.6, 4.1 and  
 147 4.1 °C, respectively) or lay close to the median (e.g., CCSM4, NorESM1-M and MIROC5  
 148 with ECS of 2.9, 2.8 and 2.7 °C, respectively).

149 Summaries of the atmospheric and ocean forcing for the two ice sheets are shown  
 150 in Figures 1 and 2, respectively. Surface warming exhibited over the AIS in CMIP6 lies  
 151 at or above the high end of the CMIP5 range. A similar pattern is evident in projected  
 152 changes in Surface Mass Balance (SMB, the annual difference between mass addition,  
 153 such as snowfall and refrozen rainfall, and mass loss, such as melt and subsequent runoff)  
 154 over the ice sheet. Neither quantity is, however, significantly higher than the CMIP5 range.  
 155 For GrIS, SMB was derived by forcing the MAR regional climate model of Greenland  
 156 (Fettweis et al., 2013) with CMIP6-derived boundary conditions. In this case, the CMIP6-  
 157 forced SMB is significantly more negative (i.e., higher GMSLR rise) than is the case for  
 158 CMIP5 forcing. Indeed, all four SSP585 ESMs fall outside the CMIP5 range and, by 2100,  
 159 anomalies from UKESM1-0-LL and CESM2 approach twice that of largest CMIP5 ESM.  
 160 The oceanic forcing of the AIS is described in detail by Jourdain et al. (2020) and for  
 161 the GrIS by Slater et al. (2020). The thermal forcing derived from the CMIP6 models  
 162 for both ice sheets lies within the range of the CMIP5 models with the exception of UKESM1-  
 163 0-LL SSP585, which is occasionally higher. In many cases, the forcing lies towards the  
 164 centre of the CMIP5 range despite the higher ECS of the CMIP6 models. As would be  
 165 expected thermal forcing from CNRM-CM6-1 SSP126 is less than that from CNRM-CM6-  
 166 1 SSP585, however the difference is similar to the difference between the four SSP585  
 167 models.

## 168 3 Summary of ISMIP6 experimental procedure

169 The procedures used to convert the climate information summarised in Figures 1  
 170 and 2 into forcing imposed on ice sheet models are summarised in a series of papers for  
 171 Antarctic ocean (Jourdain et al., 2020; Favier et al., 2019), Greenland ocean (Slater et  
 172 al., 2019, 2020) and Greenland atmosphere (Fettweis et al., 2013; Goelzer et al., 2020a).  
 173 Details of the experimental protocols employed can be found in Nowicki et al. (2016) and  
 174 Nowicki et al. (2020).

175 These protocols were primarily employed by ice sheet modelling groups to gener-  
 176 ate projections using forcing from the CMIP5 ensemble, which are reported in Goelzer  
 177 et al. (2020b) for GrIS and Seroussi et al. (2020) for AIS, however groups also conducted

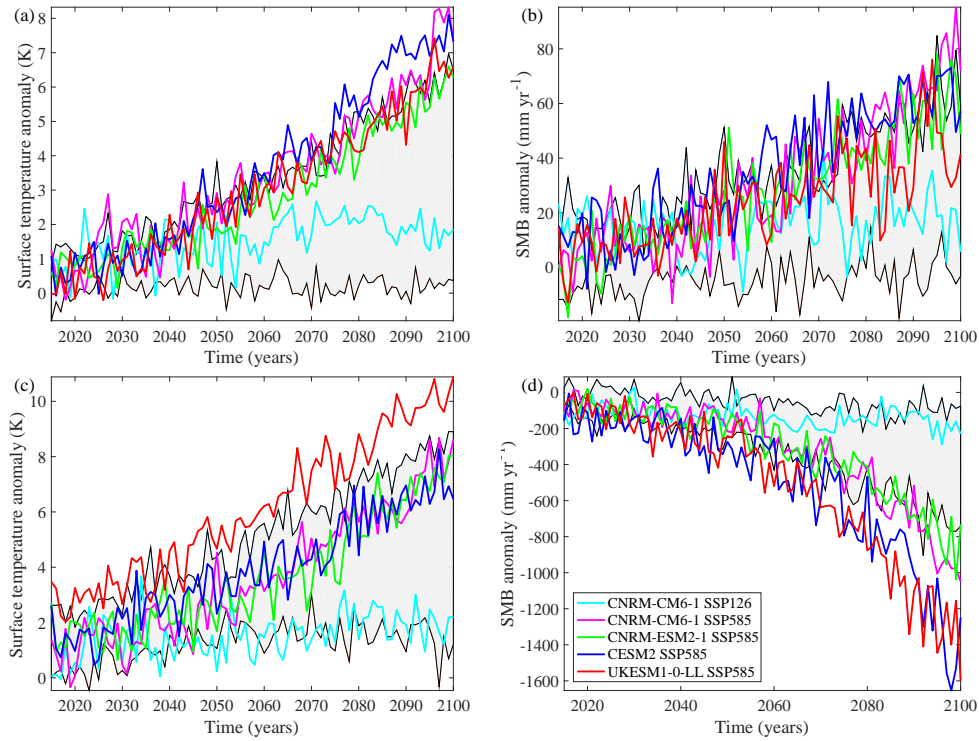


**Figure 1.** Atmospheric forcing used in CMIP6-forced experiments. (a) and (b) mean annual surface air temperature and Surface Mass Balance (SMB) anomalies over AIS. (c) and (d) mean annual surface air temperature and SMB anomaly for GrIS. Individual CMIP6 experiments are as shown as coloured lines (legend in panel (d)). Grey shading reflects range of CMIP5 forcing encompassed by all of the CMIP5 experiments used by ISMIP6 (i.e., highest and lowest CMIP5 forcing for each year).

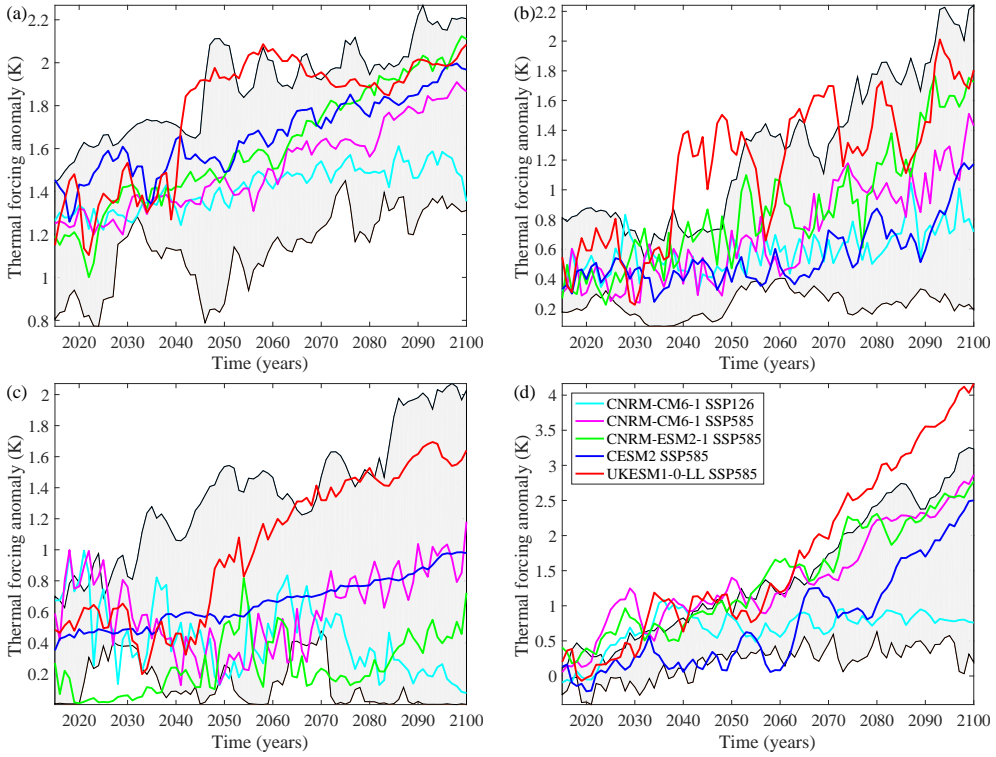


**Figure 2.** Ocean thermal forcing used in CMIP6-forced experiments for AIS sectors (a) Pine Island and Thwaites Glaciers, (b) Filchner-Ronne ice shelf, (c) Ross ice shelf and (d) for GrIS. Individual CMIP6 experiments are as shown as coloured lines (legend in panel (d)). Grey shading reflects range of CMIP5 forcing encompassed by all of the CMIP5 experiments used by ISMIP6 (i.e., highest and lowest CMIP5 forcing for each year).

**Table 1.** Overview of experiments and modelling groups participating in the CMIP6-forced exercise for AIS. Please refer to Seroussi et al. (2020) for model and group details. Symbols are those used in Figure 3.

Group	Model	Open	Standard	Symbol
AWI	PISM	1-5	1-5	○
ILTS_PIK	SICOPOLIS		1-5	△
JPL	ISSM		1-5	▷
NCAR	CISM	1-5	1-5	△
LSCE	GRISLI		1-5	□
UCIJPL	ISSM		1-5	▽
VUB	AISMPALEO		1-3	◇
Total		2	7	

**Table 2.** Overview of experiments and modelling groups participating in the CMIP6-forced exercise for GrIS. Please refer to Goelzer et al. (2020b) for model and group details. Symbols are those used in Figure 4. ‘f’ refers to filled symbol.

Group	Model	Open	Standard	Symbol
AWI	ISSM1		1-5	○
AWI	ISSM2		1-5	△
AWI	ISSM3		1-5	▷
BGC	BISICLES	1-3		*
GSFC	ISSM		1-2	□
ILTS_PIK	SICOPOLIS1		1-5	△
ILTS_PIK	SICOPOLIS2		1-5	▽
IMAU	IMAUICE2		1-3,5	◇
JPL	ISSM		1-5	○ f
JPL	ISSMPALEO		1-3,5	△ f
LSCE	GRISLI		1-5	▷ f
NCAR	CISM		1-5	□ f
UAF	PISM1		1-3,5	△ f
UAF	PISM2	1-3,5		▽ f
UCIJPL	ISSM1		1-3	◇ f
VUB	GISM		1-5	+
Total		2	14	

experiments using forcing from the CMIP6 ensemble as summarised in Tables 1 and 2. Both tables refer to experiments using the following numbering: 1) The CNRM-CM6-1 model run with scenario SSP585 (roughly equivalent to RCP8.5 of CMIP5), 2) CNRM-CM6-1 with SSP126 (roughly equivalent to RCP2.6 of CMIP5), and SSP585 with 3) UKESM1-0-LL, 4) CESM2, 5) CNRM-ESM2-1. Within the ISMIP6 design, experiments could be performed under ‘standard’ or ‘open’ configurations (see Nowicki et al., 2020). The former refers to the full implementation of ISMIP6 protocols for converting climate forcing into the mass fluxes experienced by the ice sheets, while in the latter individual groups used their own previously existing methods to do this.

## 187 4 GMSLR projections

188 Figure 3 shows projections for the AIS from the seven participating ice sheet mod-  
 189 els for each CMIP6-forced experiment along with ranges from the equivalent CMIP5-forced  
 190 experiments (Seroussi et al., 2020). Figure 3 b to d compares these projections with ranges  
 191 derived for the CMIP5 ensemble at 2100. The equivalent ranges for the whole AIS are  
 192 -14 to 155 mm for RCP2.6, and -76 to 300 mm for RCP8.5. The regional contributions  
 193 from West and East AIS are within or below the ranges reported for CMIP5 forcing. In  
 194 many cases, they sit in the lower half of this range. This, however, is likely to reflect the  
 195 high GMSLR associated with one ESM in CMIP5 ensemble of six (HadGEM2-ES), whose  
 196 projected GMSLR was typically much higher (roughly twice that of the other ESMs for  
 197 West AIS and positive rather than negative for East AIS). The projected GMSLR for  
 198 all three AIS regions for CMIP6 and CMIP5 is very compatible if HadGEM2-ES is ex-  
 199 cluded from the latter.

200 Comparing projections for SSP126 (one ESM only) and SSP585 (four ESMs) sug-  
 201 gests that there is little impact of emission scenario on projected GMSLR for AIS. This  
 202 is, again, most likely to be related to the contrasting impacts for global warming on the  
 203 ice sheet's mass budget through increases in both mass loss by ice-sheet discharge and  
 204 gain by snow accumulation.

205 The relationship between forcing and GMSLR for each CMIP6 ESM is complicated.  
 206 For instance, ocean thermal forcing (Figure 2), air temperature anomalies (Figure 1) tend  
 207 to be larger for UKESM1-0-LL; however, this is not reflected in their projected GMSLR.  
 208 This is most likely to be associated with the compensatory effect of increased precipi-  
 209 tation (Figure 1) in these ESMs.

210 Figure 4 shows projections for the GrIS from the fourteen participating ice-sheet  
 211 models for each CMIP6-forced experiment along with ranges from the equivalent CMIP5-  
 212 forced experiments (Goelzer et al., 2020b). Projected GMSLR is either at the upper end  
 213 of the CMIP5-forced range or well above it. Indeed, both CESM2 and UKESM1-0-LL-  
 214 based projections do not overlap with the CMIP5 range at all and, in the latter case, are  
 215 almost double. In contrast to the AIS, projections for SSP126 (one ESM) are consider-  
 216 ably lower than SSP585 (four ESMs) such that the ranges for CMIP6 SSP126 and SSP585  
 217 do not overlap. The trajectory of GMSLR associated with SSP126 starts to become dis-  
 218 tinct from SSP585 around 2060 but is not entirely separate until 2090. There is also a  
 219 suggestion that GMSLR may stabilise (or at least increase at a far reduced rate) beyond  
 220 2100 for SSP126, which is certainly not the case for SSP585.

## 221 5 Discussion

222 We present the first comparison between CMIP5 and CMIP6-based projections of  
 223 the contribution of ice sheets to future GMSLR up to 2100. This comparison is partic-  
 224 ularly interesting because many CMIP6 ESMs have higher climate sensitivity than their  
 225 CMIP5 counterparts (Forster et al., 2019; Meehl et al., 2020) and their projections of  
 226 future global warming are therefore higher. The comparison is hampered by the use of  
 227 a relatively small ensemble of available CMIP6 ESMs, which are all at the upper end of  
 228 CMIP6's range of climate sensitivity.

229 The comparison between CMIP5 and CMIP6 is markedly different for the two ice  
 230 sheets, reflecting the very different ways in which the ice sheets are impacted by and re-  
 231 spond to changes in the global climate system. For the GrIS, our results suggest that  
 232 GMSLR contributions under CMIP6 are much higher than for CMIP5 perhaps by a fac-  
 233 tor of two. They also suggest a significant difference between SSP585 and SSP126, with  
 234 the former experiencing accelerating rates of mass loss in marked contrast to the ten-  
 235 dency towards stabilization of the latter.

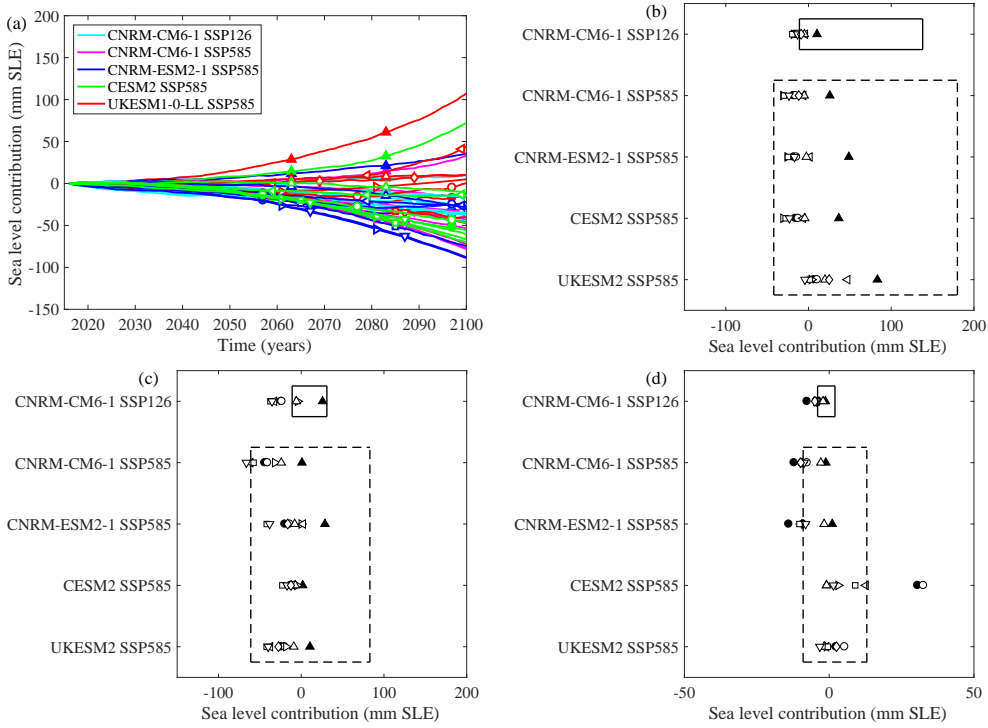


**Figure 3.** GMSLR contribution from the AIS to 2100. (a) Time series of contribution between 2015 and 2100 (in mm) for whole ice sheet as a function of ice sheet model (symbol) and experiment (see legend). Contribution at 2100 for (b) West AIS, (c) East AIS and (d) Antarctic Peninsula. Symbols refer to ice sheet models and are given in Table 1. Filled symbols refer to ‘open’ experiments and unfilled for ‘standard’. Boxes in panels (b) to (d) refer to ranges from equivalent CMIP5-forced experiments (see Seroussi et al. (2020)).

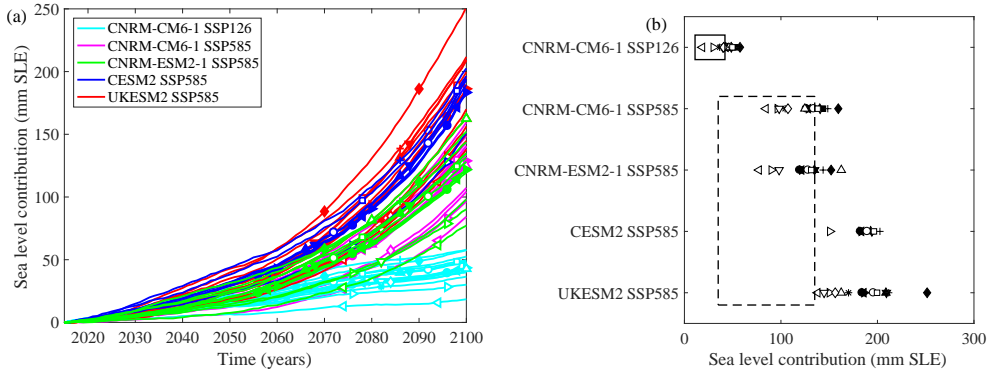


**Figure 4.** GMSLR contribution from the GrIS to 2100. (a) Time series of contribution between 2015 and 2100 (in mm) for whole ice sheet as a function of ice sheet model (symbol) and experiment (see legend) and (b) contribution at 2100. Symbols refer to ice sheet models and are given in Table 2. Boxes in panel (b) refers to ranges from equivalent CMIP5-forced experiments (see Goelzer et al. (2020b)).

236 Goelzer et al. (2020b) demonstrate that in excess of 80% of GrIS' contribution to  
 237 GMSLR can be explained by changing SMB (primarily by surface melt and subsequent  
 238 runoff), which is mostly controlled by atmospheric processes. The link between global  
 239 warming and mass loss from the ice sheet is therefore fairly direct and a strong relation-  
 240 ship between the two should be expected. The higher climate sensitivity of the sampled  
 241 CMIP6 ESMs will therefore manifest itself as a larger GMSLR contribution in compari-  
 242 son to CMIP5. It should also be noted that for GrIS (in contrast to AIS), global warm-  
 243 ing is likely to favour increased mass loss by both atmospheric (i.e., SMB) and ocean forc-  
 244 ing (i.e., discharge). However it appears that, at least within the ISMIP6 experimental  
 245 design, ocean forcing plays a secondary role to the atmosphere.

246 For AIS, our results up to 2100 suggest little difference between CMIP6 and CMIP5-  
 247 forced projections. This reflects the more complex interactions between this ice sheet and  
 248 the global climate system. Global warming is likely to favour mass loss through changes  
 249 in discharge resulting from increased ocean thermal forcing; however, the opposite is ex-  
 250 pected of the atmospheric forcing where warming is likely to favour mass gain (as a con-  
 251 sequence of increased snow accumulation). The higher climate sensitivity of the sampled  
 252 CMIP6 ESMs is therefore associated with both increased mass gain (snowfall) and mass  
 253 loss (discharge) resulting in little net change in comparison to CMIP5 forcing. The com-  
 254 plicated regional nature of interactions between ocean thermal forcing and AIS' discharge  
 255 (e.g., Jenkins et al., 2018) is also likely to weaken any link between global warming and  
 256 AIS mass loss.

257 The experimental design of the CMIP6-forced experiments reported here does not  
 258 include the fracture and collapse of AIS' floating ice shelves resulting from meltwater pond-  
 259 ing due to significant atmospheric warming (Trusel et al., 2015). This process has been  
 260 cited as a necessary precursor to rapid ice loss by the retreat of marine ice cliffs (DeConto  
 261 & Pollard, 2016). As ice shelf fracture was included in the CMIP5-forced experiments,  
 262 an initial assessment can be made by comparing the amount of atmospheric warming pro-  
 263 jected to occur under CMIP5 and CMIP6. Figure 1 suggests that CMIP6 ESMs lie close  
 264 to or above the maximum CMIP5 surface temperature warming for AIS. For CMIP5 forc-  
 265 ing, this process is limited to the Antarctic Peninsula and areas around George V ice shelf  
 266 and Totten glacier and its impact on GMSLR is ~28 mm (Seroussi et al., 2020). Ice-shelf  
 267 fracture and associated processes may therefore be important under some CMIP6 forc-  
 268 ing, in particular for CESM2 and UKESM1-0-LL, and likely be enhanced beyond 2100.

## 269 Acknowledgments

270 We would like to thank the Climate and Cryosphere (CliC) project for providing sup-  
 271 port for ISMIP6 through the sponsorship of workshops and hosting the ISMIP6 website.  
 272 We acknowledge the University at Buffalo for their help with ISMIP6 data distribution,  
 273 and the multiple agencies that support CMIP5, CMIP6 and the ESGF. This is ISMIP6  
 274 contribution number 12. This project received funding from the European Union's Hor-  
 275 izon 2020 research and innovation programme under grant agreement No 869304, PRO-  
 276 TECT contribution number 4.

## 277 References

- 278 Barthel, A., Agosta, C., Little, C. M., Hatterman, T., Jourdain, N. C., Goelzer, H.,  
 279 ... Bracegirdle, T. J. (2020). Cmip5 model selection for ismip6 ice sheet  
 280 model forcing: Greenland and antarctica. *The Cryosphere*, 14, 855–879. doi:  
 281 10.5194/tc-14-855-2020
- 282 DeConto, R., & Pollard, D. (2016). Contribution of antarctica to past and future  
 283 sea-level rise. *Nature*, 531(7596), 591-597. doi: 10.1038/nature17145
- 284 Eyring, V., Bony, S., Meehl, G. A., Senior, C. A., Stevens, B., Stouffer, R. J., &  
 285 Taylor, K. E. (2016). Overview of the coupled model intercomparison project

- phase 6 (cmip6) experimental design and organization. *Geosci. Model Dev.*, 9(5), 1937–1958. doi: 10.5194/gmd-9-1937-2016
- Favier, L., Jourdain, N. C., Jenkins, A., Merino, N., Durand, G., Gagliardini, O., ... Mathiot, P. (2019). Assessment of sub-shelf melting parameterisations using the ocean–ice-sheet coupled model nemo(v3.6)–elmer/ice(v8.3). *Geosci. Model Dev.*, 12, 2255–2283. doi: 10.5194/gmd-12-2255-2019
- Fettweis, X., Franco, B., Tedesco, M., van Angelen, J. H., Lenaerts, J. T. M., van den Broeke, M. R., & Gallée, H. (2013). Estimating the greenland ice sheet surface mass balance contribution to future sea level rise using the regional atmospheric climate model mar. *The Cryosphere*, 7(2), 469–489. doi: 10.5194/tc-7-469-2013
- Flato, G., Marotzke, J., Abiodun, B., Braconnot, P., Chou, S., Collins, W., ... Rummukainen, M. (2013). Evaluation of climate models. In T. Stocker et al. (Eds.), *Climate change 2013: The physical science basis. contribution of working group i to the fifth assessment report of the intergovernmental panel on climate change* (p. 741–866). Cambridge, United Kingdom and New York, NY, USA: Cambridge University Press. doi: 10.1017/CBO9781107415324.020
- Forster, P., Maycock, A., McKenna, C., & Smith, C. (2019). Latest climate models confirm need for urgent mitigation. *Nature Climate Change*.
- Goelzer, H., Noel, B., Edwards, T. L., Fettweis, X., Gregory, J. M., Lipscomb, W. H., ... van den Broeke, M. R. (2020a). Remapping of greenland ice sheet surface mass balance anomalies for large ensemble sea-level change projections. *The Cryosphere*, 14(6), 1747–1762. doi: 10.5194/tc-14-1747-2020
- Goelzer, H., Nowicki, S., Payne, A., Larour, E., Seroussi, H., Lipscomb, W., ... van den Broeke, M. (2020b). The future sea-level contribution of the greenland ice sheet: a multi-model ensemble study of ismip6. *The Cryosphere*, 14(9), 3071–3096. doi: 10.5194/tc-14-3071-2020
- IPCC. (2013). Annex iii: Glossary. In T. Stocker et al. (Eds.), *Climate change 2013: The physical science basis. contribution of working group i to the fifth assessment report of the intergovernmental panel on climate change* (p. 1447–1466). Cambridge, United Kingdom and New York, NY, USA: Cambridge University Press. doi: 10.1017/CBO9781107415324.031
- Jenkins, A., Shoosmith, D., Dutrieux, P., Jacobs, T. W., Stan Kim, Lee, S. H., Ha, H. K., & Stammerjohn, S. (2018). West antarctic ice sheet retreat in the amundsen sea driven by decadal oceanic variability. *Nature Geoscience*, 11(10), 733–738. doi: 10.1038/s41561-018-0207-4
- Jourdain, N., Asay-Davis, X., Hattermann, T., Straneo, F., Seroussi, H., Little, C., & Nowicki, S. (2020). A protocol for calculating basal melt rates in the ismip6 antarctic ice sheet projections. *The Cryosphere*, 14(9), 3111–3134. doi: 10.5194/tc-14-3111-2020
- Meehl, G., Senior, C., Eyring, V., Flato, G., Lamarque, J.-F., Stoffer, R., & Schlund, M. (2020). Context for interpreting equilibrium climate sensitivity and transient climate response from the cmip6 earth system models. *Science Advances*, 6(26). doi: 10.1126/sciadv.aba1981
- Nowicki, S., Goelzer, H., Seroussi, H., Payne, A. J., Lipscomb, W. H., Abe-Ouchi, A., ... van de Wal, R. (2020). Experimental protocol for sea level projections from ismip6 standalone ice sheet models. *The Cryosphere*, 14(7), 2331–2368. doi: 10.5194/tc-14-2331-2020
- Nowicki, S., Payne, A., Larour, E., Seroussi, H., Goelzer, H., Lipscomb, W., ... Shepherd, A. (2016). Ice sheet model intercomparison project (ismip6) contribution to cmip6. *Geoscientific Model Development*, 9(12), 4521–4545. doi: 10.5194/gmd-9-4521-2016
- Schoof, C. (2007). Ice sheet grounding line dynamics: Steady states, stability, and hysteresis. *Journal of Geophysical Research-Earth Surface*, 112(F3). doi: 10.1029/2006JF000664

- 341 Seroussi, H., Nowicki, S., Payne, A. J., Goelzer, H., Lipscomb, W. H., Abe-Ouchi,  
342 A., ... Zwinger, T. (2020). Ismip6 antarctica: a multi-model ensemble of the  
343 antarctic ice sheet evolution over the 21st century. *The Cryosphere*, 14(9),  
344 3033–3070. doi: 10.5194/tc-14-3033-2020
- 345 Slater, D. A., Felikson, D., Straneo, F., Goelzer, H., Little, C., Morlighem, M., ...  
346 Nowicki, S. (2020). 21st century ocean forcing of the greenland ice sheet for  
347 modeling of sea level contribution. *The Cryosphere*, 14(3), 985–1008. doi:  
348 10.5194/tc-14-985-2020
- 349 Slater, D. A., Straneo, F., Felikson, D., Little, C. M., Goelzer, H., Fettweis,  
350 X., & Holte, J. (2019). Estimating greenland tidewater glacier retreat  
351 driven by submarine melting. *The Cryosphere*, 13(9), 2489–2509. doi:  
352 10.5194/tc-13-2489-2019
- 353 Taylor, K., Stouffer, R., & Meehl, G. (2012). An overview of cmip5 and the ex-  
354 periemnt design. *Bulletin of the American Meteorological Society*, 93(4), 485-  
355 498. doi: 10.1175/BAMS-D-11-00094.1
- 356 Trusel, L. D., Frey, K. E., Das, S. B., Karnauskas, K. B., Kuipers Munneke, P., van  
357 Meijgaard, E., & van den Broeke, M. R. (2015). Divergent trajectories of  
358 antarctic surface melt under two twenty-first-century climate scenarios. *Nature  
359 Geoscience*, 8(12), 927-932. doi: 10.1038/ngeo2563